THE JOURNAL OF BIOLOGICAL CHEMISTRY VOL. 284, NO. 34, pp. 22633–22640, August 21, 2009

The Interaction of Mitochondrial Iron with Manganese Superoxide Dismutase*[S]

Received for publication, May 28, 2009, and in revised form, June 24, 2009 Published, JBC Papers in Press, June 27, 2009, DOI 10.1074/jbc.M109.026773

Amornrat Naranuntarat[‡1], Laran T. Jensen[‡], Samuel Pazicni[§], James E. Penner-Hahn[§], and Valeria C. Culotta[‡2]

From the [‡]Department of Environmental Health Sciences, Johns Hopkins University Bloomberg School of Public Health, Baltimore, Maryland 21205 and the [§]Department of Chemistry, University of Michigan, Ann Arbor, Michigan 48109

Superoxide dismutase 2 (SOD2) is one of the rare mitochondrial enzymes evolved to use manganese as a cofactor over the more abundant element iron. Although mitochondrial iron does not normally bind SOD2, iron will misincorporate into *Saccharomyces cerevisiae* Sod2p when cells are starved for manganese or when mitochondrial iron homeostasis is disrupted by mutations in yeast *grx5*, *ssq1*, and *mtm1*. We report here that such changes in mitochondrial manganese and iron similarly affect cofactor selection in a heterologously expressed *Escherichia coli* Mn-SOD, but not a highly homologous Fe-SOD. By x-ray absorption near edge structure and extended x-ray absorption fine structure analyses of isolated mitochondria, we find that misincorporation of iron into yeast Sod2p does not correlate with significant changes in the average oxidation state or coordination chemistry of bulk mitochondrial iron. Instead, small changes in mitochondrial iron are likely to promote iron-SOD2 interactions. Iron binds Sod2p in yeast mutants blocking late stages of iron-sulfur cluster biogenesis (*grx5*, *ssq1*, and *atm1*), but not in mutants defective in the upstream Isu proteins that serve as scaffolds for iron-sulfur biosynthesis. In fact, we observed a requirement for the Isu proteins in iron inactivation of yeast Sod2p. Sod2p activity was restored in *mtm1* and *grx5* mutants by depleting cells of Isu proteins or using a dominant negative Isu1p predicted to stabilize iron binding to Isu1p. In all cases where disruptions in iron homeostasis inactivated Sod2p, we observed an increase in mitochondrial Isu proteins. These studies indicate that the Isu proteins and the iron-sulfur pathway can donate iron to Sod2p.

Metal-containing enzymes are generally quite specific for their cognate cofactor. Misincorporation of the wrong metal ion can be deleterious and tends to be a rare occurrence in biology. A prime example of metal ion selectivity is illustrated by the family of manganese- and iron-containing superoxide dismutases (SODs)[3]. This large family of enzymes utilizes either manganese or iron as cofactors to scavenge superoxide anion. The iron- and manganese-containing forms are highly homologous to one another at primary, secondary, and tertiary levels and have virtually identical metal binding and catalytic sites (1–3). Despite this extensive homology, Mn- and Fe-SODs are only active with their cognate metal. Misincorporation of iron into Mn-SOD or vice versa alters the redox potential of the enzyme's active site and prohibits superoxide disproportionation (4, 5). Nevertheless, misincorporation of iron into Mn-SOD does occur *in vivo* (6, 7). The isolated Mn-SOD from *Escherichia coli* is found as a mixture of manganese- and iron-bound forms (7); binding of manganese is favored under oxidative stress, whereas iron binding is increased under anaerobic conditions (3, 8). It has been proposed that changes in bioavailability of manganese *versus* iron determine the metal selectivity of Mn-SOD in bacterial cells (3, 8). But is this also true for Fe-SOD? Currently, there is no documentation of manganese misincorporation into Fe-SOD *in vivo*.

Unlike bacteria that co-express Mn- and Fe-SOD molecules in the same cell, eukaryotic mitochondria generally harbor only one member of the Fe/Mn-SOD family, a tetrameric Mn-SOD typically known as SOD2 (9). In some organisms, SOD2 is essential for survival (10–12), and mitochondria have therefore evolved to prevent iron-SOD2 interactions despite high levels of mitochondrial iron relative to manganese. Using a yeast model system, we have shown previously that metal ion misincorporation can occur with *Saccharomyces cerevisiae* Sod2p (7). Specifically, iron binds and inactivates yeast Sod2p when cells are either starved for manganese or have certain disruptions in mitochondrial iron homeostasis. These disruptions include mutations in *MTM1*, a mitochondrial carrier protein that functions in iron metabolism (7, 13), and mutations in *GRX5* or *SSQ1*, involved in iron-sulfur biogenesis (14). We proposed that these disruptions lead to expansion of a mitochondrial pool of so-called SOD2-reactive iron (7). Currently, it is unknown whether SOD2-reactive iron represents a major shift in the chemistry of bulk mitochondrial iron or whether it is just a small pool of the metal emerging from one or more specific sites.

The *grx5* and *ssq1* mutants that promote iron-SOD2 interactions encode just two of many components of a complex pathway

* This work was supported, in whole or in part, by National Institutes of Health Grants ES-08996 (to V. C. C.) and GM-38047 (awarded to J. E. P.-H.) and the Johns Hopkins University NIEHS Center.

[S] The on-line version of this article (available at http://www.jbc.org) contains supplemental "Experimental Procedures," Tables S1 and S2, and Figs. S1 and S2.

[1] Supported by a scholarship from the Royal Thai government.

[2] To whom correspondence should be addressed: Division of Toxicology, Dept. of Environmental Health Sciences, The Johns Hopkins University Bloomberg School of Public Health, Baltimore, MD 21205. Tel.: 410-955-3029; Fax: 410-955-0116; E-mail: vculotta@jhsph.edu.

[3] The abbreviations used are: SOD, superoxide dismutase; XANES, x-ray absorption near edge structure; EXAFS, extended x-ray absorption fine structure; BPS, bathophenanthrolinedisulfonate; WT, wild type; KD, knockdown.

for iron-sulfur biogenesis (15, 16). One of the key components is a well conserved iron-sulfur scaffold protein originally described for bacteria as IscU, also known as mammalian ISCU and *S. cerevisiae* Isu1p and Isu2p, referred collectively herein as "Isu proteins" (17–22). The iron-sulfur clusters on Isu proteins are labile and can be transferred to target iron-sulfur proteins through the aid of mitochondrial factors including Grx5p and Ssq1p (15, 16). It is not clear whether disruption of the iron-sulfur pathway *per se* is sufficient to promote iron interactions with yeast Sod2p or whether this effect is specific to *grx5*, *ssq1*, and *mtm1* mutants.

In the current study, we explore the nature of mitochondrial iron that can interact with Sod2p. We find that the changes in mitochondrial metal homeostasis that shift metal binding in yeast Sod2p likewise alter metal cofactor selection in a heterologously expressed Mn-SOD, but not in a Fe-SOD molecule. Through x-ray absorption near edge structure (XANES) and extended x-ray absorption fine structure (EXAFS) analyses of mitochondrial iron, we detected no major change in bulk mitochondrial iron under conditions that promote iron-SOD2 interactions. SOD2-reactive iron appears to represent a small pool of the metal, and we provide evidence that the iron-sulfur scaffold Isu1p can act as an important source of this reactive iron.

EXPERIMENTAL PROCEDURES

Yeast Strains and Culture Conditions—The strains employed in this study are isogenic to either BY4741 (*MAT***a**, *leu2*Δ*0*, *met15*Δ*0*, *ura3*Δ*0*, and *his3*Δ*1*) or BY4742 (*MAT*α, *leu2*Δ*0*, *lys2*Δ*0*, *ura3*Δ*0*, and *his3*Δ*1).* Strains include the previously reported MY019 (*mtm1*Δ::*LEU2*) (7), *MY020 (mtm1*Δ::*LEU2 sod2*Δ::*kanMX4*) (7), *and LJ109 (rho*$^-$) (23). Single gene deletions strains in the BY4741 background 5278 (*ssq1*Δ::*kanMX4*), 2769 (*grx5*Δ::*kanMX4*), 1878 (*smf2*Δ::*kanMX4*), and 12482 (BY4742 *isu2*Δ::*kanMX4*) were obtained from Research Genetics, Inc. Strain AN008 (*yfh1*Δ::*LEU2*) is a derivative of the *yfh1*Δ::*URA3* strain MY036 (7), where *URA3* was replaced with *LEU2*. Strain LJ206 (*atm1*Δ::*URA3*) was created with the *atm1*Δ disruption plasmid pLJ170 (described below). The p*GAL-ISU1* knock down strain LJ403 (*isu1*Δ::kanMX4, *isu2*Δ::HIS3, p*GAL-ISU1*) was created by deleting *isu2* with pLJ318 (described below) in the *isu1*Δ::kanMX4 strain expressing *ISU1* under *GAL1* (plasmid pLJ386; described below). The p*MET3-ISU1* knockdown strain LJ436 (BY4742 *isu2*Δ::*kanMX4*, p*MET3-ISU1*::*HIS3*) was created by integrating the *MET3* promoter just prior to the *ISU1* coding sequence using plasmid pLJ472 (described below) in a strain also harboring a *isu2*Δ deletion. *MTM1* and *GRX5* were deleted in BY4742 and LJ436 using plasmids pVC257 (13) and pLJ190 (described below) respectively generating strains LJ443 (*mtm1*Δ::*LEU2*), LJ444 (*mtm1*Δ::*LEU2 isu2*Δ::*kanMX4*, p*MET3-ISU1*::*HIS3*), LJ445 (*grx5*Δ::*URA3*), and LJ446 (*grx5*Δ::*URA3, isu2*Δ::*kanMX4*, p*MET3-ISU1*::*HIS3*).

Yeast cells were grown either in enriched yeast extract, peptone-based medium supplemented with 2% glucose (YPD), 2% galactose (YPGal), 3% glycerol (YPG), or in synthetic defined medium. To minimize oxidative damage in iron accumulating yeast strains, stocks of cells were maintained in oxygen-depleted culture jars (GasPak, Becton Dickinson), and liquid cultures were grown without aeration.

Plasmids—The *S. cerevisiae SOD2* expressing vector pAN001 was created by mobilizing *SOD2* sequences −552 to +889 from pEL111 (13) through SalI and BamHI digestion and by ligation into the *CEN URA3* vector pRS316 (24). pAN002 expresses *E. coli sodA* fused to the *SOD2* mitochondrial targeting signal and gene promoter. For this, *sodA* sequences +1 to +625 were PCR-amplified with NdeI and BglII sites and ligated to a derivative of pEL111 with a NdeI site engineered at +78 in yeast *SOD2* in which *SOD2* sequences +78 to +700 were removed by NdeI/BglII digestion. The pKL-SOD plasmid for expressing FLAG-tagged *E. coli* Fe-SOD was a generous gift from Dr. Jerry Kaplan, University of Utah (25, 26). To create the *atm1*Δ::*URA3* plasmid pLJ170 for deleting *ATM1* sequences +60 to +1,541, *ATM1* fragments −493 to +60 and +1,541 to +2,566 mobilized through EcoRI/BglII and EcoRI/KpnI digestion were inserted into KpnI/BamHI-digested pRS306 (*URA3*). The *grx5*Δ::*URA3* plasmid pLJ190 was generated by PCR-amplifying upstream (−703 to −232) and downstream sequences (+416 to +855) of *GRX5* introducing EcoRI and SpeI (upstream) or KpnI and EcoRI (downstream) restriction sites. Following digestion the PCR products were ligated into KpnI/SpeI digested pRS306 (*URA3*). To generate pLJ129 expressing *ISU1* under *PGK1*, the coding sequence for *ISU1* was PCR-amplified with BamHI and SalI sites and inserted into these sites of pLJ150 (*URA3* 2 μm containing the *PGK1* promoter and *CYC1* terminator). Plasmid pLJ357 is a derivative of pLJ129 expressing D71A *ISU1* generated by QuikChange mutagenesis (Stratagene). To create the *GAL1*-driven *ISU1* vector pLJ386, the BamHI-SalI *ISU1*-containing fragment of pLJ129 was inserted into these same sites of pYC2/CT harboring the *GAL1* promoter (*URA3 CEN*) (Invitrogen). The *isu2*Δ::*HIS3* disruption plasmid pLJ388 was created by inserting the *isu2* disruption cassette from pSG101 (18) into the BamHI-SalI sites of pRS403. The p*MET3-ISU1* promoter replacement plasmid was generated by PCR-amplifying *ISU1* upstream (−929 to −343) and downstream (+1 to +687) sequences introducing NotI and SacI (upstream) or SphI and NotI (downstream) restriction sites and *MET3* sequences (−425 to −3) introducing BamHI and SphI sites. Following digestion the *MET3* promoter and *ISU1* downstream sequences were ligated into pRS313 (*HIS3*) digested with BamHI/NotI producing plasmid pLJ469. The p*MET3-ISU1* (downstream) fusion was then excised with BamHI/NotI and ligated together with the *ISU1* upstream sequences digested with NotI/SacI into pRS403 (*HIS3*) digested with BamHI/SacI. The resulting plasmid pLJ472 was linearized with NotI and used to replace the *ISU1* promoter with the methionine-repressible *MET3* promoter.

Analysis of SOD Activity and Immunoblots—Whole cell lysates of *S. cerevisiae* strains were prepared by glass bead homogenization (27) from cells that were grown in liquid cultures of either YPD or synthetic defined medium to late log. For glucose repression of *GAL-ISU1* and methionine repression of p*MET3-ISU1*, cells were maintained on solid YPD for at least 48 h prior to 14–16 h in liquid YPD cultures. The lysates were analyzed for SOD activity by native gel electrophoresis and nitroblue tetrazolium staining (13) and for immunoblot analysis by denaturing gel electrophoresis using antibodies directed against SOD2 (27) or *E. coli* IscU that recognizes yeast Isu1p

and Isu2p (18). Quantitation of SOD activity bands utilized ImageQuant TL (version 2005) software (GE Healthcare). Immunoblots were visualized by ECL detection (Amersham Pharmacia Biotech) or by the Odyssey infrared imaging system (Licor Biosciences). Immunoblots were quantitated by either ImageQuant TL software (version 2005) for ECL or Odyssey software (version 1.2).

Miscellaneous Biochemical Analyses—For measurements of total mitochondrial iron, crude mitochondria were prepared as described previously (23) from 100-ml YPD cultures, and iron measurements were carried out on a PerkinElmer Life Sciences AAnalyst 600 graphite furnace atomic absorption spectrometer according to published methods (23). For XANES and EXAFS analysis, cells were cultured for 16 h in YPD to an A_{600} 4.0–4.5 and mitochondria were isolated from duplicate 2.0 liter cultures as above in buffers containing 1 mM dithiothreitol. The yield of protein was typically 10–20 μg/μl. 40 μl of each mitochondrial sample was transferred to Lucite cuvettes for x-ray absorption spectra data collection as described in the supplemental "Experimental Procedures".

RESULTS

Mitochondrial Iron Homeostasis Effects on Heterologous SODs—We have shown previously that cofactor selectivity in mitochondrial Sod2p is greatly influenced by mitochondrial manganese and iron homeostasis (7). We tested whether such effects of the mitochondrial environment are limited to eukaryotic SOD2 or can be extended to other members of the Fe/Mn-SOD family. In the experiment of Fig. 1, *E. coli* Mn-SOD was expressed in yeast mitochondria using the *S. cerevisiae SOD2* gene promoter and mitochondrial targeting signal. *E. coli* Mn-SOD shows activity in wild type (WT) yeast mitochondria that was not inhibited by increasing mitochondrial iron through iron supplements (Fig. 1*A*, *lanes 4* and *5*). Thus, as with yeast Sod2p, *E. coli* Mn-SOD seems largely nonreactive to high mitochondrial iron from WT cells. Yet, iron does react with *E. coli* Mn-SOD in the *mtm1*, *ssq1*, and *grx5* mutants that also inactivate yeast Sod2p. As seen in Fig. 1*B*, *E. coli* Mn-SOD activity is lost in *mtm1*, *ssq1*, and *grx5* mutants (*lanes 3–5*), and activity is restored by depleting iron through chelation with BPS (bathophenanthrolinedisulfonate) (*lanes 6–8*). BPS treatments also somewhat increased activity of *E. coli* Mn-SOD and yeast Sod2p expressed in WT cells (Fig. 1*C*, *lanes 2* and *4*), consistent with a low level of iron reactivity with these SODs even in WT cells (7). The mitochondrial environment has the same impact on cofactor selection in a heterologous Mn-SOD from bacteria as is seen with the endogenous yeast Sod2p.

We tested whether the mitochondrial environment can likewise influence cofactor selection in an Fe-SOD. When expressed in WT yeast mitochondria, Fe-SOD from *E. coli* is active, consistent with iron binding (Fig. 2*A*, *lane 2*). To determine whether a fraction of the enzyme is inactivated by manganese binding, Fe-SOD was expressed in the mitochondria of *smf2*Δ mutants that accumulate very low manganese (7, 27). Fe-SOD activity was not significantly elevated in this manganese-starved cell (Fig. 2*A*, *lane 3*), indicating that mitochondrial

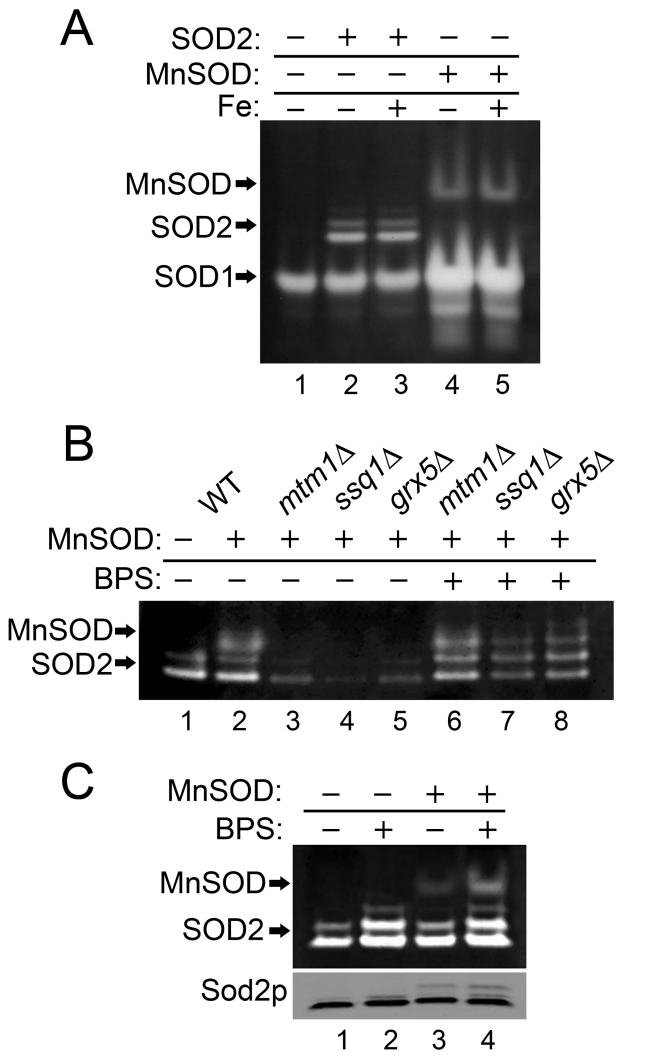

FIGURE 1. **Effects of mitochondrial iron homeostasis on a heterologous *E. coli* Mn-SOD.** The designated strains were grown in YPD medium supplemented where indicated with 80 μM BPS or 2 mM ammonium iron(III) citrate (*Fe:*+). Whole-cell lysates were analyzed for SOD activity by native gel electrophoresis and nitroblue tetrazolium staining. Mn-SOD, SOD1, and SOD2 indicate positions of active Mn-SOD from *E. coli* and Cu/Zn-Sod1p and manganese Sod2p from *S. cerevisiae*, respectively. Sod2p polypeptide from the whole-cell lysates was analyzed by immunoblot (*C*, *bottom panel*). Strains utilized: the *sod2*Δ strain transformed where indicated with the yeast *SOD2* plasmid pAN001 (*A*) or the *E. coli* Mn-SOD expression plasmid, pAN002 (*B* and *C*). The BY4741 WT (*B*, *lanes 1* and *2*, and *C*) or indicated mutant derivatives (*B*) transformed where designated (+) with plasmid pAN002 for expressing *E. coli* Mn-SOD.

manganese is not binding the enzyme. Fe-SOD activity was also largely unchanged by the same *mtm1* and *ssq1* mutants that favor iron binding to Mn-SOD over manganese (Fig. 2*B*, *lane 3* and *4*). Even when yeast cells are overloaded with manganese, Fe-SOD retains its activity. As seen in Fig. 2*C*, the same manganese treatments that promote manganese binding and manganese activation of yeast Sod2p (*top*) had no effect on Fe-SOD activity (*bottom*). Fe-SOD is largely refractory to the changes in metal homeostasis that affect cofactor selection in Mn-SOD molecules. Although mitochondrial iron is normally quite bioavailable for Fe-SOD, this is not the case for Mn-SOD. Only a specialized pool of mitochondrial iron, such as that expanded in *mtm1*, *grx5*, and *ssq1* mutants, can gain access to manganese SOD molecules.

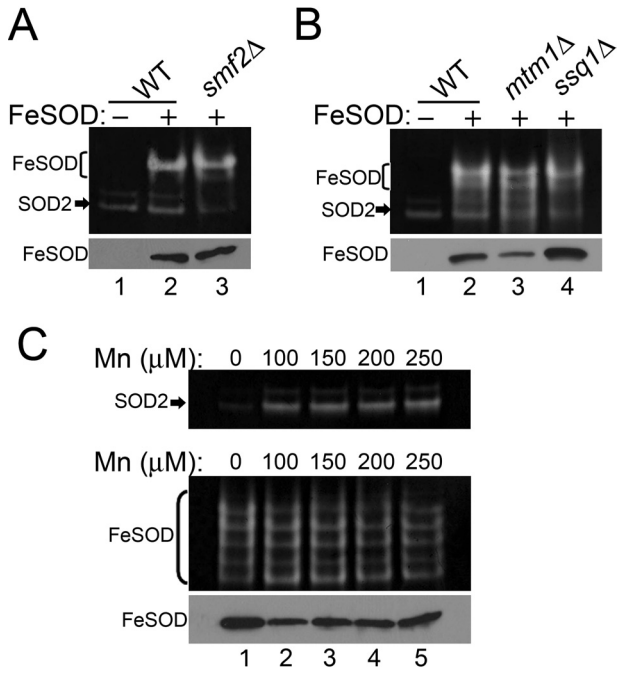

FIGURE 2. **Enzymatically active Fe-SOD expressed in yeast mitochondria.** Strains that were transformed where indicated (*Fe-SOD:+*, *A* and *B*, and *C*, *bottom panel*) with the plasmid for expressing a FLAG-tagged version of *E. coli* Fe-SOD were analyzed for SOD activity (*top*) and for levels of Fe-SOD by immunoblotting with anti-FLAG (*bottom*). FLAG-tagged Fe-SOD typically runs as multiple bands on native gels; the major bands are shown in *brackets*. *S. cerevisiae* SOD2 activity is shown by *arrows*. Strains utilized: *WT*, BY4741; *smf2*Δ, 1878 (*A*); *WT*, BY4741; *mtm1*Δ, MY019; *ssq1*Δ, 5278 (*B*); *mtm1*Δ, MY019 (*top panel*); *sod2*Δ *mtm1*Δ, MY020 (*C*, *bottom panel*) transformed with the *E. coli* Fe-SOD expression plasmid.

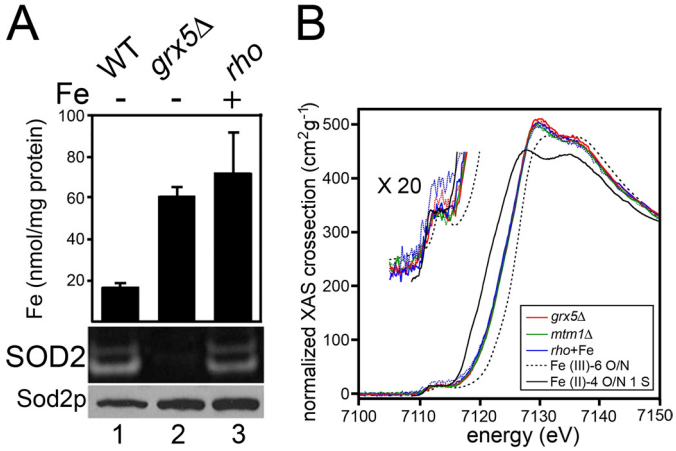

FIGURE 3. **Bulk mitochondrial iron is unchanged in cells accumulating SOD2-reactive iron.** *A*, the designated strains grown where indicated in the presence of 2 mM ammonium iron(III) citrate were subjected to analysis of mitochondrial iron by atomic absorption spectrometry (values represent averages of four readings from two independent cultures, error bars indicate S.D.) (*top*) and to yeast Sod2 activity analysis (*middle*) and Sod2p protein levels (*bottom*) as in Fig. 1. *B*, normalized XANES spectra of mitochondria samples (*grx5*Δ, *mtm1*Δ, and *rho* supplemented with 2 mM ammonium iron(III) citrate; *rho*+*Fe*). Duplicate sample sets from independent cultures are color-coded per the *inset legend*, with each duplicate represented by a *solid* and *dotted line*. The expansion showing the 1*s* → 3*d* transition is enlarged 20-fold vertically. Strains utilized: *WT*, BY4741; *grx5*Δ, 2769; *mtm1*Δ, MY019; *rho*$^-$, LJ109.

Bulk Mitochondrial Iron Is Not Affected in Yeast Mutants Where Iron Binds Sod2p—The mitochondrial iron that accumulates in *grx5*, *ssq1*, and *mtm1* mutants would appear to be of a unique nature in that it readily reacts with Mn-SOD molecules. To address whether these mutants are associated with a bulk change in the average oxidative state and/or coordination environment of mitochondrial iron, we employed XANES and EXAFS. Such spectroscopy has previously been used to analyze mitochondrial iron of mammalian cells defective for frataxin (28), which, in our analogous yeast *yfh1* mutants, does not react with SOD2. Because our interests lie in "SOD2-reactive iron," we analyzed the mitochondrial iron of yeast *grx5*Δ and *mtm1*Δ mutants, as well as a *rho* mutant control (*grx5* and *mtm1* cells are *rho*$^-$; (29)). When treated with iron, the *rho* strain accumulates high mitochondrial iron that does not react with or inactivate Sod2p, whereas the isogenic *grx5*Δ mutant does exhibit iron activation of Sod2p (Fig. 3*A*). EXAFS spectra were measured from duplicate samples as described previously (30) to k = 12 Å^{-1} (supplemental Tables S1 and S2 and Fig. S1). Spectra were fit using Feff 7.02 parameters over the k range 2–9 Å^{-1}. As seen in Fig. 3*B*, the normalized (31) XANES spectra for the *grx5*Δ and *mtm1*Δ mutants and the *rho* control are identical, indicating that there is no detectable change in either the average iron oxidation state or geometry. The edge energy is consistent with an approximately equal mixture of Fe(II) and Fe(III) and the weak 1*s*-3*d* intensity indicates that the bulk of the iron has ~octahedral symmetry. Although the absolute Fe(II):Fe(III) ratio cannot be discerned because the apparent ratio depends on the reference spectra used for Fe(II) and Fe(III), it is nevertheless clear that there is no significant change in oxidation state in mitochondrial iron from *grx5* and *mtm1*Δ *versus* the *rho* control. A conversion of >5% of the iron from Fe(II) to Fe(III) or vice versa would be readily detectable. The EXAFS spectra (supplemental Fig. S1) were fit using a single iron-oxygen/nitrogen shell. Again, there was no significant change in spectra of *grx5*, *mtm1*, and the *rho* control; in all three cases, the apparent iron-oxygen distance was 1.97–2.00 Å, consistent with the expected $R_{Fe\text{-}O}$ for 6-coordinate Fe(III). Overall, iron inactivation of Sod2p does not correlate with major changes in total mitochondrial iron. The pool of mitochondrial iron that inactivates SOD2 may represent a small fraction.

Effects of Blocking Specific Steps in Iron-Sulfur Biogenesis on Sod2p—Clues to understanding the origin of SOD2-reactive iron may come from an analysis of the iron-sulfur pathway. The yeast *grx5* and *ssq1* mutations that promote iron inactivation of Sod2p block both mitochondrial and cytosolic iron-sulfur biogenesis (16). A factor needed for cytosolic, but not mitochondrial, iron-sulfur clusters is yeast *ATM1*, the homologue to mammalian ABCB7 (32, 33). Previously, knockdown of human ABCB7 was associated with a lowering of SOD2 activity (34), and we now provide evidence that this reflects iron inactivation of the enzyme. As seen in Fig. 4*A*, deletion of *S. cerevisiae ATM1* results in a dramatic rise in mitochondrial iron. This iron is reacting with Sod2p as there is a pronounced loss in Sod2p activity (Fig. 4*B*, *lane 2*) that was rescued by iron chelation (*lane 3*).

Another component of the iron-sulfur biogenesis pathway is the yeast Isu proteins (also known as IscU in bacteria and ISCU in mammals) onto which labile iron-sulfur scaffolds are built (17–22, 35). A combined deletion in *S. cerevisiae ISU1* and *ISU2* is lethal (18, 35); hence we expressed *ISU1* under the repressible

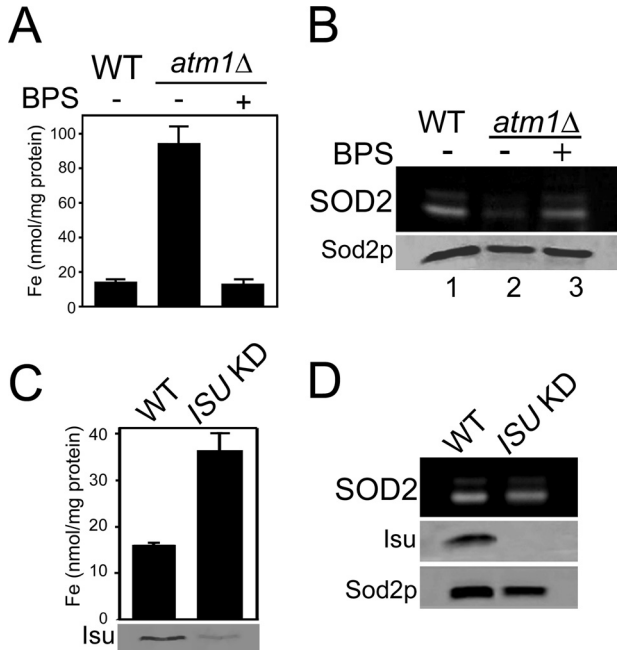

FIGURE 4. **Effects of disrupting iron-sulfur biogenesis on Sod2p activity.** *A* and *B*, the designated strains were grown in YPD medium containing where indicated (*BPS:* +) 80 μM BPS. *A*, mitochondrial iron levels were measured as in 3*A*. *B*, Sod2p activity and protein levels were monitored as in Fig. 1. *C* and *D*, cells that were originally maintained on galactose-containing medium were shifted to glucose for 48 h to deplete Isu1p in the ISU knockdown (*KD*) cultures. *C*, *top*, mitochondrial iron levels monitored as in 3*A*. *C*, *bottom*, and *D*, whole-cell lysates were analyzed where indicated for Isu (combination of yeast Isu1p and Isu2p) protein levels by immunoblot and for Sod2p activity and protein as in Fig. 1. Strains utilized: *WT*, BY4741; *atm1*Δ, LJ206 (*A* and *B*); *WT*, BY4741; *ISU KD*, LJ403 (*C* and *D*).

S. cerevisiae GAL1 promoter in a *isu1*Δ *isu2*Δ background. Repression of *ISU1* resulted in an increase in mitochondrial iron (Fig. 4*C*) as previously shown with *isu* deficiency and with loss of *mtm1*, *grx5*, and *ssq1* (13, 17, 18, 36–38). However, in the case of *isu* loss, the elevated iron did not impair Sod2p activity; there was no evidence of iron interactions with the enzyme (Fig. 4*D*, *lane 2*).

As a second approach to yeast Isu protein inactivation, we sought to obtain a dominant negative Isu1p. Recently, Dean and colleagues (39, 40) created a dominant negative (D39A) IscU from *Azotobacter vinelandii* that can bind iron and assemble an iron-sulfur cluster but cannot transfer this cluster to recipient iron-sulfur proteins. Iron binding is very stable compared with the labile iron binding of wild type IscU. We created the analogous D71A in *S. cerevisiae* Isu1p (Fig. 5*A*). Expression of D71A Isu1p in WT cells rapidly caused the cells to become petite or respiratory deficient, and this defect was not reversed upon subsequent loss of the D71A *ISU1* expression plasmid (Fig. 5*B*), consistent with permanent mitochondrial DNA damage (*rho* mutations). Rapid loss of mitochondrial DNA is typically seen in yeast cells defective in iron-sulfur biogenesis (17, 23, 36, 41–43). Despite this dominant negative effect of D71A Isu1p on WT mitochondria, there was no loss in Sod2p activity (Fig. 5*D*, *lane 3*). Together with the *ISU1* down-regulation study of Fig. 4*D*, these studies show that the iron accumulating in Isu deficient cells does not react with Sod2p. It is not a loss of iron-sulfur biogenesis *per se* that creates SOD2-reactive iron

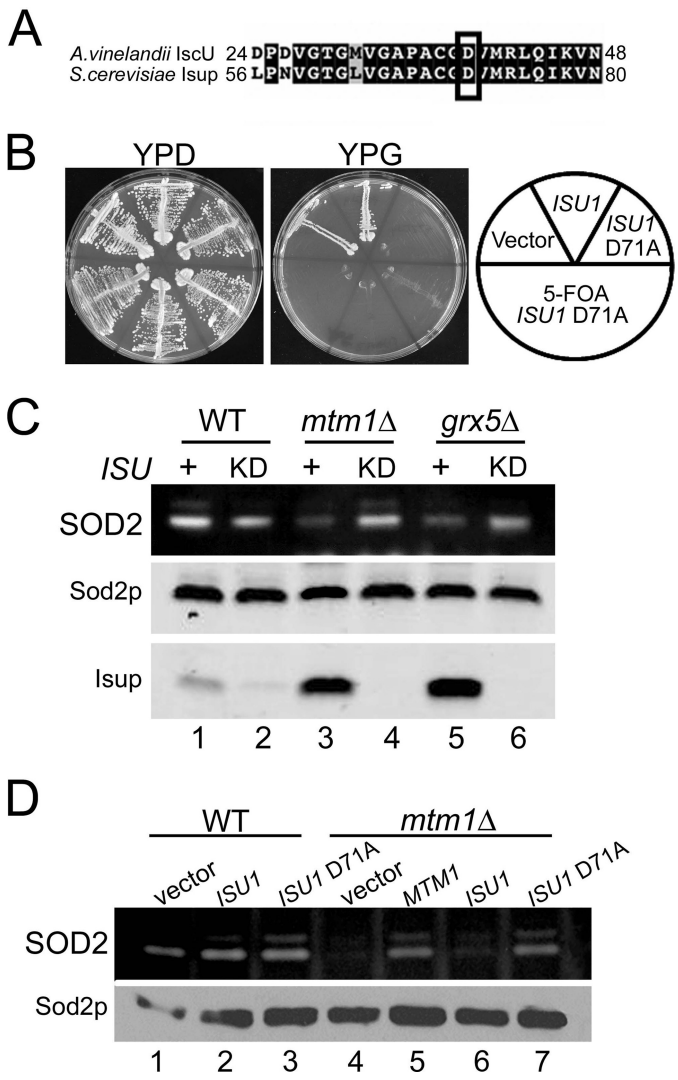

FIGURE 5. **Blocking Isu activity in yeast.** *A*, alignment of an N-terminal segment of *A. vinelandii* IscU *versus S. cerevisiae* Isu1p. Identical and similar residues are in *black* and *gray*; *boxed* is a conserved aspartate targeted for mutagenesis. *B*, WT cells transformed with vectors for overproducing either WT Isu1p or D71A Isu1p or with empty vector were tested for growth on fermentable (YPD) and nonfermentable (YPG) carbon sources, the latter being a marker of mitochondrial respiration. Where indicated (+5-fluoroorotic acid), three independent transformants for D71A *ISU1* were induced to shed the D71A *ISU1* plasmid by growth on 5-fluoroorotic acid prior to growth tests. *C* and *D*, whole-cell lysates were analyzed for SOD activity (*top*) and Sod2p protein levels (*bottom*) as in Fig. 1. *C*, cells that were originally maintained on methionine-free medium were shifted to enriched methionine-containing YPD medium for 48 h to deplete Isu1p in the ISU KD cultures. *ISU* +, cells harboring wild type *ISU1* and *ISU2* alleles. *Isup*, combined levels of Isu1p and Isu2p detected by immunoblot using an anti-*E. coli* IscU antibody. *D*, WT and *mtm1*Δ cells were transformed with the indicated plasmids for overexpression of wild type or D71A *ISU1* or for *MTM1* and were grown in selecting synthetic defined medium. Strains utilized: *WT*, BY4741 and *mtm1*Δ, MY019 (*A*, *B*, and *D*); *WT*, BY4742; *ISU KD*, LJ436 (*C*); *mtm1*Δ, LJ443; *mtm1*Δ *ISU KD*, LJ444; *grx5*Δ, LJ445; *grx5*Δ *ISU KD*, LJ446.

but rather specific blockages in the pathway (*e.g. grx5*, *ssq1*, and *atm1* mutants).

Isu as a Potential Source of SOD2-reactive Iron—We reported previously that in *mtm1*Δ mutants, iron inactivation of Sod2p can be reversed by a deletion in *YFH1* encoding iron binding frataxin (7). Because Yfh1p can donate iron to Isu molecules (44), we tested whether loss of the yeast Isu proteins can similarly prevent iron-Sod2p interactions. First, the Isu pro-

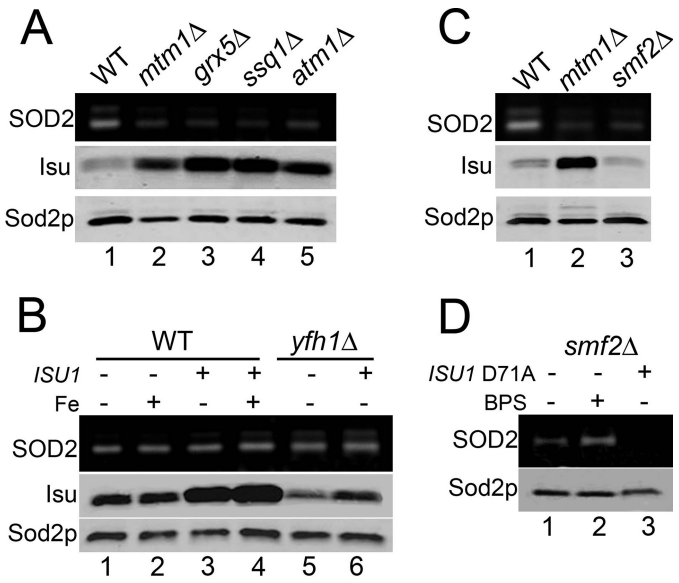

FIGURE 6. **Isu1p levels and iron inactivation of Sod2p.** Sod2p activity and protein levels and Isu protein levels were monitored as in Fig. 5. *A* and *C*, indicated strains were grown in YPD medium. *B* and *D*, strains were grown in selecting synthetic defined medium supplemented where indicated with 2 mM ammonium iron(III) citrate (*Fe:*+) or 80 μM BPS. As designated (*ISU1*: + or *ISU1* D71A: +), cells were transformed with the pLJ129 or pLJ357 vectors for overexpressing WT or D71A Isu1p. Strains utilized: *WT*, BY4741; *mtm1*Δ, MY019; *grx5*Δ, 2769; *ssq1*Δ, 5278; *atm1*Δ, LJ206; *yfh1*Δ, AN015; *smf2*Δ, 1878.

teins were depleted by placing the chromosomal *ISU1* gene under control of the methionine-repressible *MET3* protein in an *isu2*Δ strain. As seen in Fig. 5*C*, growth of this strain in enriched (methionine-containing) medium resulted in a major loss of total Isu proteins (*lanes 2*, *4*, and *6*; *bottom*). In the background of a *mtm1*Δ or *grx5*Δ strain, such depletion of Isu resulted in restoration of Sod2p activity (Fig. 5*C*, *lanes 4* and *6*; see also supplemental Fig. S2). Hence, total loss of Isu proteins can disrupt the trafficking of iron toward Sod2p. To address this further, we exploited the dominant negative D71A Isu1p described above that is expected to bind, but not transfer iron (39, 40). As seen in Fig. 5*D*, overexpression of D71A *ISU1*, but not WT *ISU1*, reversed loss of Sod2p activity in *mtm1* mutants (*lane 7*). The Isu polypeptides are present in this case but are presumably unable to release iron, indicating that iron derived from Isu1p can react with Sod2p.

ISU1 is known to be up-regulated in *ssq1*Δ (45, 46) and *grx5*Δ cells (47), and we now report that *mtm1*Δ strains show a similar increase in Isu protein levels, as do *atm1*Δ mutants that likewise exhibit iron-inactivation of Sod2p (Fig. 6*A* and supplemental Fig. S2). In contrast, Isu protein levels do not increase in our *yfh1*Δ strain that hyperaccumulates a form of iron that does not react with Sod2p (Fig. 6*B*, *lane 5*). There appears to be a close correlation between Isu levels and the degree of Sod2p inactivation (supplemental Fig. S2). Nevertheless, elevating Isu protein levels alone is not sufficient to promote iron binding to Sod2p. Overexpression of *ISU1* in WT or *yfh1*Δ cells did not cause Sod2p inactivation, even when cells were treated with iron supplements (Fig. 6*B*, *lanes 3*, *4*, and *6*). Specific disruptions in iron homeostasis are required.

We have shown previously that iron can gain access to Sod2p without disruptions in mitochondrial iron if the cells are starved for manganese (7). Yeast *smf2*Δ mutants accumulate very low manganese but normal iron (7). These cells show a loss in Sod2p activity similar to effects seen in *mtm1* mutants (Fig. 6*C*). However, in this case, Sod2p inactivation is not associated with increased Isu protein levels (Fig. 6*C*, *lane 3*). Moreover, Sod2p activity in *smf2*Δ mutants was not rescued by the dominant negative D71A Isu1p (Fig. 6*D*, *lane 2*) even though iron chelation treatments did improve activity (*lane 3*). Therefore Isu1p is not responsible for the inactivation of Sod2p under conditions of manganese starvation.

DISCUSSION

In eukaryotic mitochondria, iron atoms outnumber manganese by nearly two orders of magnitude (7). Iron is also more widely used as cofactor, including roughly 15 heme and iron-sulfur containing proteins (48) compared with only one or two manganese-containing enzymes. Eukaryotic Sod2p is one of those rare mitochondrial enzymes that has chosen manganese over iron. Yet even so, slippage of the wrong metal can occur, and we have shown that the enzyme switches from the active manganese bound state to the inactive iron-state with specific disruptions in mitochondrial iron homeostasis. The switch in cofactor selection is not caused by a global change in the chemical environment of mitochondrial iron. Rather, a fraction of mitochondrial iron becomes highly reactive with Sod2p, and we have identified the iron-sulfur scaffold protein Isu as one potential source of this reactive iron.

The effects of the mitochondrial environment on Sod2p cofactor selection were reproduced with a heterologous bacterial Mn-SOD expressed in mitochondria. In fact, the impact of the mitochondria on metal selectivity of Mn-SOD was similar to what has previously been reported for this bacterial enzyme expressed in its native host (6, 8). We therefore propose that manganese SOD molecules from bacteria to eukaryotes have evolved to capture manganese based on differential bioavailability of manganese *versus* iron rather than a specific manganese-metallochaperone.

Although manganese SOD molecules are highly susceptible to changes in metal bioavailability, the same is not true for the highly homologous Fe-SOD from *E. coli*. When expressed in mitochondria, Fe-SOD exists in the active iron-bound state and is refractory to the changes in manganese and iron homeostasis that dictate metal specificity in Mn-SOD. The affinity constants of Fe-SOD for manganese or iron have not been reported; however, it is possible that the affinity for iron over manganese is sufficiently high to preclude mis-incorporation of the less abundant manganese. Our findings with Fe-SOD have also shed light into the bulk mitochondrial iron that does not typically react with Mn-SOD. What we have denoted previously as the "SOD2-inert iron" (7) may in fact be quite bioavailable but just in a form that cannot compete with manganese for binding to Mn-SOD molecules.

We have identified the iron-sulfur scaffold protein Isu as a potential source for SOD2-reactive iron. Depletion of the yeast Isu polypeptides or expression of a dominant negative D71A Isu1p reversed iron inactivation of Sod2p in *mtm1*Δ and *grx5*Δ cells. Based on studies with the highly homologous bacterial IscU proteins, iron binding to wild type Isu proteins is quite

labile, facilitating ready transfer of iron to iron-sulfur proteins (21). But in cases where such iron transfer cannot be completed (*e.g.* yeast *grx5*, *ssq1*, and *atm1* mutants affecting downstream steps in iron-sulfur biogenesis), the levels of Fe-bound Isu increase in the cell (14). A fraction of this labile iron may then be diverted to Sod2p. In *yfh1*Δ strains that block an upstream step in iron-sulfur biogenesis, mitochondrial iron should not accumulate on Isu proteins and accordingly, we observed no iron inactivation of Sod2p in our *yfh1*Δ mutants (7). Although iron binding to wild type Isu is labile, iron binding to Asp71 (or the analogous position in bacterial IscU) mutants is stable (39, 40), explaining the ability of yeast D71A Isu1p to reverse Sod2-inactivation in *mtm1*Δ mutants.

Although the function of Mtm1p is not yet known, we predict *mtm1* mutations affect the iron-sulfur biogenesis pathway. In many regards, *mtm1*Δ mutations phenocopy *grx5* and *ssq1* mutants defective in iron-sulfur synthesis including increases in mitochondrial iron (13), induction of the Aft1 iron regulon (7), loss of Sod2p activity (7) and induction of Isu (this study). In our recent studies with a severe knockdown of *mtm1* through *MET3* transcriptional repression, we observed a loss of iron-sulfur aconitase activity without a loss in mitochondrial DNA.[4] Furthermore, recent studies of zebrafish and mammalian orthologues to yeast Mtm1p also implicate a role in mitochondrial iron homeostasis consistent with effects on iron-sulfur biogenesis (49). Based on its ability to phenocopy yeast *grx5* and *ssq1* mutants, Mtm1p may participate in a downstream component of iron-sulfur biogenesis yet to be determined.

Lastly, it is worth noting that Isu and the iron-sulfur pathway are not the sole source of iron for Sod2p inactivation. In the absence of iron homeostasis defects, a small pool of yeast Sod2p can react with iron, and this pool is expanded when cells are starved for manganese (7). In this case, Isu proteins are not responsible for Sod2p inactivation, and it is likely that other labile iron sources in the mitochondria, *e.g.* iron-sulfur proteins, may be involved.

Acknowledgments—We thank Jerry Kaplan for the Fe-SOD expression plasmid, Larry Vickery for anti-IscU, and Dennis Dean for helpful discussions. XAS spectra measured at the Stanford Synchrotron Radiation Lightsource, a national user facility operated by Stanford University on behalf of the U. S. Dept. of Energy, Office of Basic Energy Sciences. The Stanford Synchrotron Radiation Laboratory Structural Molecular Biology Program is supported by the Department of Energy, Office of Biological and Environmental Research, and by the National Institutes of Health, National Center for Research Resources, Biomedical Technology Program.

REFERENCES

1. Wintjens, R., Noël, C., May, A. C., Gerbod, D., Dufernez, F., Capron, M., Viscogliosi, E., and Rooman, M. (2004) *J. Biol. Chem.* **279,** 9248–9254
2. Carlioz, A., Ludwig, M. L., Stallings, W. C., Fee, J. A., Steinman, H. M., and Touati, D. (1988) *J. Biol. Chem.* **263,** 1555–1562
3. Whittaker, J. W. (2003) *Biochem. Soc. Trans.* **31,** 1318–1321
4. Vance, C. K., and Miller, A. F. (1998) *J. Am. Chem. Soc.* **120,** 461–467
5. Vance, C. K., and Miller, A. F. (2001) *Biochemistry* **40,** 13079–13087
6. Beyer, W. F., Jr., and Fridovich, I. (1991) *J. Biol. Chem.* **266,** 303–308
7. Yang, M., Cobine, P. A., Molik, S., Naranuntarat, A., Lill, R., Winge, D. R., and Culotta, V. C. (2006) *EMBO J.* **25,** 1775–1783
8. Privalle, C. T., and Fridovich, I. (1992) *J. Biol. Chem.* **267,** 9140–9145
9. Weisiger, R. A., and Fridovich, I. (1973) *J. Biol. Chem.* **248,** 4793–4796
10. Lebovitz, R. M., Zhang, H., Vogel, H., Cartwright, J., Jr., Dionne, L., Lu, N., Huang, S., and Matzuk, M. M. (1996) *Proc. Natl. Acad. Sci. U.S.A.* **93,** 9782–9787
11. Duttaroy, A., Paul, A., Kundu, M., and Belton, A. (2003) *Genetics* **165,** 2295–2299
12. Kirby, K., Hu, J., Hilliker, A. J., and Phillips, J. P. (2002) *Proc. Natl. Acad. Sci. U.S.A.* **99,** 16162–16167
13. Luk, E., Carroll, M., Baker, M., and Culotta, V. C. (2003) *Proc. Natl. Acad. Sci. U.S.A.* **100,** 10353–10357
14. Mühlenhoff, U., Gerber, J., Richhardt, N., and Lill, R. (2003) *EMBO J.* **22,** 4815–4825
15. Rouault, T. A., and Tong, W. H. (2005) *Nat. Rev. Mol. Cell Biol.* **6,** 345–351
16. Lill, R., and Mühlenhoff, U. (2005) *Trends Biochem. Sci.* **30,** 133–141
17. Gerber, J., Neumann, K., Prohl, C., Mühlenhoff, U., and Lill, R. (2004) *Mol. Cell. Biol.* **24,** 4848–4857
18. Garland, S. A., Hoff, K., Vickery, L. E., and Culotta, V. C. (1999) *J. Mol. Biol.* **294,** 897–907
19. Tong, W. H., and Rouault, T. A. (2006) *Cell Metab.* **3,** 199–210
20. Zheng, L., Cash, V. L., Flint, D. H., and Dean, D. R. (1998) *J. Biol. Chem.* **273,** 13264–13272
21. Agar, J. N., Krebs, C., Frazzon, J., Huynh, B. H., Dean, D. R., and Johnson, M. K. (2000) *Biochemistry* **39,** 7856–7862
22. Agar, J., Zhneg, L., Cash, V., Dean, D., and Johnson, M. (2000) *J. Am. Chem. Soc.* **122,** 2136–2137
23. Jensen, L. T., and Culotta, V. C. (2000) *Mol. Cell. Biol.* **20,** 3918–3927
24. Sikorski, R. S., and Hieter, P. (1989) *Genetics* **122,** 19–27
25. Balzan, R., Agius, D. R., and Bannister, W. H. (1999) *Biochem. Biophys. Res. Comm* **256,** 63–67
26. Shaw, G. C., Cope, J. J., Li, L., Corson, K., Hersey, C., Ackermann, G. E., Gwynn, B., Lambert, A. J., Wingert, R. A., Traver, D., Trede, N. S., Barut, B. A., Zhou, Y., Minet, E., Donovan, A., Brownlie, A., Balzan, R., Weiss, M. J., Peters, L. L., Kaplan, J., Zon, L. I., and Paw, B. H. (2006) *Nature* **440,** 96–100
27. Luk, E. E., and Culotta, V. C. (2001) *J. Biol. Chem.* **276,** 47556–47562
28. Popescu, B. F., Pickering, I. J., George, G. N., and Nichol, H. (2007) *J. Inorg. Biochem.* **101,** 957–966
29. Laliberté, J., Whitson, L. J., Beaudoin, J., Holloway, S. P., Hart, P. J., and Labbé, S. (2004) *J. Biol. Chem.* **279,** 28744–28755
30. Tobin, D. A., Pickett, J. S., Hartman, H. L., Fierke, C. A., and Penner-Hahn, J. E. (2003) *J. Am. Chem. Soc.* **125,** 9962–9969
31. Weng, T. C., Waldo, G. S., and Penner-Hahn, J. E. (2005) *J. Synchrotron. Radiat.* **12,** 506–510
32. Kispal, G., Csere, P., Guiard, B., and Lill, R. (1997) *FEBS Lett.* **418,** 346–350
33. Bekri, S., Kispal, G., Lange, H., Fitzsimons, E., Tolmie, J., Lill, R., and Bishop, D. F. (2000) *Blood* **96,** 3256–3264
34. Cavadini, P., Biasiotto, G., Poli, M., Levi, S., Verardi, R., Zanella, I., Derosas, M., Ingrassia, R., Corrado, M., and Arosio, P. (2007) *Blood* **109,** 3552–3559
35. Schilke, B., Voisine, C., Beinert, H., and Craig, E. (1999) *Proc. Natl. Acad. Sci. U.S.A.* **96,** 10206–10211
36. Rodríguez-Manzaneque, M. T., Tamarit, J., Bellí, G., Ros, J., and Herrero, E. (2002) *Mol. Biol. Cell* **13,** 1109–1121
37. Jensen, L. T., Sanchez, R. J., Srinivasan, C., Valentine, J. S., and Culotta, V. C. (2004) *J. Biol. Chem.* **279,** 29938–29943
38. Lesuisse, E., Knight, S. A., Courel, M., Santos, R., Camadro, J. M., and Dancis, A. (2005) *Genetics* **169,** 107–122
39. Raulfs, E. C., O'Carroll, I. P., Dos Santos, P. C., Unciuleac, M. C., and Dean, D. R. (2008) *Proc. Natl. Acad. Sci. U.S.A.* **105,** 8591–8596
40. Unciuleac, M. C., Chandramouli, K., Naik, S., Mayer, S., Huynh, B. H., Johnson, M. K., and Dean, D. R. (2007) *Biochemistry* **46,** 6812–6821
41. Kispal, G., Csere, P., Prohl, C., and Lill, R. (1999) *EMBO J.* **18,** 3981–3989
42. Mühlenhoff, U., Richhardt, N., Ristow, M., Kispal, G., and Lill, R. (2002) *Hum. Mol. Genet.* **11,** 2025–2036
43. Babcock, M., de Silva, D., Oaks, R., Davis-Kaplan, S., Jiralerspong, S., Montermini, L., Pandolfo, M., and Kaplan, J. (1997) *Science* **276,**

[4] L. T. Jensen and V. C. Culotta, unpublished observations.

1709–1712
44. Gerber, J., Mühlenhoff, U., and Lill, R. (2003) *EMBO Rep* **4,** 906–911
45. Knieszner, H., Schilke, B., Dutkiewicz, R., D'Silva, P., Cheng, S., Ohlson, M., Craig, E. A., and Marszalek, J. (2005) *J. Biol. Chem.* **280,** 28966–28972
46. Andrew, A. J., Song, J. Y., Schilke, B., and Craig, E. A. (2008) *Mol. Biol. Cell* **19,** 5259–5266
47. Bellí, G., Molina, M. M., García-Martínez, J., Pérez-Ortín, J. E., and Herrero, E. (2004) *J. Biol. Chem.* **279,** 12386–12395
48. Hudder, B. N., Morales, J. G., Stubna, A., Münck, E., Hendrich, M. P., and Lindahl, P. A. (2007) *J. Biol. Inorg. Chem.* **12,** 1029–1053
49. Nilsson, R. H., Schultz, I. J., Pierce, E. L., Soltis, K. A., Naranuntarat, A., Ward, D. M., Baughman, J. M., Paradkar, P. N., Kingsley, P. D., Culotta, V. C., Kaplan, J., Palis, J., Paw, B. H., and Mootha, V. K. (2009) *Cell Metab.*, in press